Title

Altered cerebral perfusion in executive, affective, and motor networks during adolescent depression.

Permalink

Journal

Authors

Ho, Tiffany
Wu, Jing
Shin, David
et al.

Publication Date

DOI

Peer reviewed

NIH-PA Author Manuscript

NIH-PA Author Manuscript

NIH-PA Author Manuscript

Altered Cerebral Perfusion in Executive, Affective, and Motor Networks During Adolescent Depression

Dr. Tiffany C. Ho, Ph.D.,
The University of California, San Francisco

Dr., Mr. Jing Wu, B.S.,
The University of California, San Francisco, The University of Colorado, Denver and Health Sciences Center

Dr. David D. Shin, Ph.D.,
The University of California, San Diego; The Center of Functional Magnetic Resonance Imaging

Dr. Thomas T. Liu, Ph.D.,
The University of California, San Diego; The Center of Functional Magnetic Resonance Imaging

Dr. Susan F. Tapert, Ph.D.,
The University of California, San Diego; Psychiatry Service, Veterans Affairs San Diego Health Care System

Dr., Mr. Guang Yang, B.S.,
The University of California, San Francisco; The University of California, San Diego

Dr. Colm G. Connolly, Ph.D.,
The University of California, San Francisco

Dr. Guido K.W. Frank, M.D.,
The University of Colorado, Denver and Health Sciences Center

Dr. Jeffrey E. Max, MBBCh.,
The University of California, San Diego; Rady Children's Hospital

Dr. Owen Wolkowitz, M.D.,
The University of California, San Francisco

Correspondence to Tony T. Yang, M.D., Ph.D., 401 Parnassus Avenue, San Francisco, CA 94131; tony.yang@ucsf.edu.

Supplemental material cited in this article is available online.

Dr. Stuart Eisendrath, M.D.,
The University of California, San Francisco

Dr. Fumiko Hoeft, M.D., Ph.D.,
The University of California, San Francisco

Mr. Dipavo Banerjee, B.S.,
The University of California, San Diego

Dr. Korey Hood, Ph.D.,
The University of California, San Francisco

Dr. Robert L. Hendren, D.O.,
The University of California, San Francisco

Dr. Martin P. Paulus, M.D.,
The University of California, San Diego

Dr. Alan N. Simmons, Ph.D., and
The University of California, San Diego; Psychiatry Service, Veterans Affairs San Diego Health
Care System

Dr. Tony T. Yang, M.D., Ph.D.
The University of California, San Francisco; The University of California, San Diego

Abstract

Objective—While substantial literature has reported regional cerebral blood flow (rCBF)
abnormalities in adults with depression, these studies commonly necessitated the injection of
radioisotopes into subjects. The recent development of arterial spin labeling (ASL), however,
allows for noninvasive measurements of rCBF. Currently, no published ASL studies have
examined cerebral perfusion in adolescents with depression. Thus, the aim of the present study
was to examine baseline cerebral perfusion in adolescent depression using a newly developed ASL
technique: pseudocontinuous arterial spin labeling (PCASL).

Method—25 medication-naive adolescents (ages 13–17 years) diagnosed with major depressive
disorder (MDD) and 26 well-matched controls underwent functional magnetic resonance imaging.
Baseline rCBF was measured via a novel PCASL method that optimizes tagging efficiency.

Results—Voxel-based whole brain analyses revealed significant frontal, limbic, paralimbic, and
cingulate hypoperfusion in the group with depression ($p<0.05$, corrected). Hyperperfusion was
also observed within the subcallosal cingulate, putamen, and fusiform gyrus ($p<0.05$, corrected).
Similarly, region-of-interest analyses revealed amygdalar and insular hypoperfusion in the group
with depression, as well as hyperperfusion in the putamen and superior insula ($p<0.05$, corrected).

Conclusions—Adolescents with depression and healthy adolescents appear to differ on rCBF in
executive, affective, and motor networks. Dysfunction in these regions may contribute to the
cognitive, emotional, and psychomotor symptoms commonly present in adolescent depression.
These findings point to possible biomarkers for adolescent depression that could inform early
interventions and treatments and establishes a methodology for using PCASL to noninvasively
measure rCBF in clinical and healthy adolescent populations.

Keywords

Introduction

Major depressive disorder (MDD) is associated with significant morbidity and mortality, and is one of the leading causes of disability in the United States,[1] with incidence rates rising dramatically after puberty.[2] The estimated lifetime prevalence of MDD in adolescents is over 15%,[3] with a two- to fourfold risk of depression continuing into adulthood.[4] Given the severity and pervasiveness of this disorder, understanding the underlying neural mechanisms involved in adolescent MDD is critical to developing early interventions and improving current treatments.

Functional neuroimaging studies have provided key insights into the neurobiological circuitry of MDD. Much of this earlier work measured baseline cerebral blood flow (CBF) and glucose metabolism using positron emission tomography (PET) and single photon emission computer tomography (SPECT) in adults with depression.[5–9] Both PET and SPECT, however, are highly invasive, less widely available, and notable more expensive due to having radioactive material as imaging agents, thus making these methods not appropriate for pediatric psychiatry research.[10] Consequently, functional magnetic resonance imaging (fMRI) utilizing blood oxygenation level dependent (BOLD) and arterial spin labeling (ASL) techniques has become an increasingly popular tool for noninvasively measuring brain activation in neuropsychiatric populations (for reviews on these two methods, see Detre *et al.*, 2009;[11] Greicius, 2008;[12] Brown *et al.*, 2007;[13] Fox and Raichle, 2007[14]).

Resting state fMRI studies of adults with depression[15–21] and adolescents[21–23] have examined functional connectivity patterns (i.e., temporal correlations in blood-oxygen-level-dependent [BOLD] signal) among brain regions during periods of rest. In these studies, adult MDD appears to be associated with altered functional connectivity in fronto-limbic,[19] fronto-striatal,[16] cingulate-limbic,[15,17,18,21] and limbic-paralimbic[20] networks. Similarly, resting state functional connectivity studies in adolescents[21–23] with MDD have observed aberrant connectivity between portions of the subcallosal cingulate and prefrontal,[21–23] limbic, and paralimbic sites.[22, 23] These results suggest that MDD is an illness with a distributive effect over the executive and affective networks of the brain. However, while functional connectivity analyses of BOLD resting state data can be used to identify intrinsic networks of the brain and how connective strengths within and across such networks change with depression,[12,14] these assessments are nevertheless based on correlations between BOLD time series.[10,12] The BOLD signal itself is a relative measure that is also dependent on vascular factors such as blood flow and blood volume, which can further confound interpretation.[10] Thus, even though BOLD resting state functional connectivity can reveal which correlations between brain regions or networks may be abnormal in patients with depression, it cannot provide in absolute, physiological terms which brain regions specifically are dysfunctional during depression.[10,12,24]

The ASL signal, on the other hand, is derived from the subtraction of tagged (via magnetically labeled arterial water) and control images that is directly proportional to perfusion changes (for reviews on ASL methodology, see Detre and Wang, 2002;[10] Bokkers *et al.*, 2010;[25] Borogovac and Asllani, 2012[26]). Hence, one methodological advantage of ASL over BOLD techniques is that it can provide an absolute estimate of regional CBF (rCBF) in physiological units (milliliters of blood per 100 grams of tissue per minute).[11,25] The benefit of obtaining an absolute physiological measurement like rCBF is that it could complement brain measures from other imaging modalities, such as BOLD fMRI, which are sensitive to blood flow. Additionally, perfusion patterns hold promise as objective biomarkers for tracking illness progression, pharmacological effects, and developmental brain maturation in a variety of neuropsychiatric and developmental disorders.[13,26]

Assessing whether rCBF patterns deviate significantly from the norm in at-risk groups could also potentially aid in early diagnosis, intervention, and prevention.[27] Moreover, several of the working models of adult depression that have led to the advancement of innovative treatments are based on PET studies.[6,28–32] It is therefore important to compare these findings with analogous measures in youth with depression to generate similar models that could lead to the development of further treatment options for adolescent MDD. Thus, the ability of ASL to quantify an absolute physiological measurement like PET,[11,25] yet to do so noninvasively makes it an exceptionally powerful tool for investigating brain differences between pediatric psychiatric and healthy populations.[10]

To our knowledge, there are currently no ASL-based studies examining cerebral perfusion in adolescent depression. ASL studies of adult MDD have noted perfusion differences in fronto-limbic-cingulate-striatal networks, but have reported both increased and attenuated rCBF perfusion, particularly in the limbic, paralimbic, and striatal areas.[33–36] These disparate results are further complicated by the fact that these studies recruited primarily medicated patients.[33–36] Different antidepressants could have augmenting or abating effects on rCBF, hence obscuring inferences about the baseline perfusion profiles of MDD.[37–38] Applying ASL techniques in medication-naïve individuals with depression may therefore help resolve the inconsistencies in the extant literature and determine whether hyper- or hypoperfusion is indeed a potential biomarker of adolescent MDD.

Our study was therefore designed to compare rCBF patterns in a sizeable group of nonmedicated MDD and well-matched healthy control (HCL) adolescents. The current study is notable for at least three reasons. Firstly, this is at present the only ASL study of adolescent depression. Secondly, all of the adolescents with depression in our study met full criteria for MDD, were medication naïve, and were diagnosed with minimal comorbidities at the time of scanning. Lastly, we employed a novel ASL method— pseudocontinuous arterial spin labeling (PCASL)—that optimizes tagging efficiency,[39] yields relatively high quality CBF images, and is capable of being implemented on clinical scanners.[40,41] We conducted a voxel-based whole brain analysis in order to compare rCBF levels between both groups. Given the contrary perfusion results within the limbic, paralimbic, and striatal regions in studies on adults with depression,[5–9, 15–18] we also performed a region-of-interest (ROI) analysis specifically targeting the amygdala, insula, and striatum. These structures have been shown in a variety of fMRI studies[42–45] to be heavily involved in affective processing and emotional regulation, and as such, theorized to be principal nodes within network models of depression and thus, motivating our ROI analyses.[7]

Despite developmental differences between adults and adolescents, clinical and neurobiological studies have suggested some continuity between adolescent and adult MDD.[46] Given the current paucity of perfusion studies on adolescent MDD, our hypotheses are driven primarily by PET and ASL work in adult depression.[5–9,33–36] Based on these data, MDD is thought to be characterized by abnormalities in frontal areas supporting executive functioning and in limbic, paralimbic, and cingulate regions supporting affective processing[7]—particularly, the amygdala, insula, and anterior and subcallosal cingulate— with the most consistent findings across the literature being abnormal frontal hypoperfusion and subcallosal cingular hyperperfusion in MDD.[5–9, 33–36] We therefore hypothesized that these areas would exhibit significant differences in rCBF levels between MDD and HCL adolescents and more specifically, that adolescents with MDD would exhibit frontal hypoperfusion and subcallosal cingular hyperperfusion.

Method

Subjects

Fifty-one right-handed adolescents (ages 13–17 years old) participated in the study: 25 adolescents with a current primary *DSM-IV* diagnosis of MDD (age: Mean ± SD: 15.98 ± 1.5 years; 7 males) and 26 HCL adolescents (16.42 ± 1.0 years; 7 males). Subject groups were equivalent on major demographic variables (see Table S1, available online, or Results for more details). This study was approved by the Institutional Review Boards at the University of California–San Diego, the University of California–San Francisco, Rady Children's Hospital, and the County of San Diego.

Adolescents with depression were recruited from adolescent psychiatric and primary care clinics in San Diego, while healthy controls were recruited from the same geographic area via e-mail, internet, or flyers. Male and female adolescents from all ethnicities were eligible to participate. All participating adolescents provided written informed assent and their parents/legal guardian(s) provided written informed consent in accordance with the Declaration of Helsinki. All participants received financial compensation.

The Schedule for Affective Disorders and Schizophrenia for School-Age Children–Present and Lifetime Version (KSADS-PL)[47] was administered to all potentially adolescents with depression. All KSADS-PL diagnoses were determined by a board certified child and adolescent psychiatrist. All MDD subjects in the study met full criteria for a primary diagnosis of MDD and were excluded if they had a primary psychiatric diagnosis other than MDD. None of our MDD subjects were diagnosed with a comorbid disruptive disorder. However, due to the high rate of comorbidity of MDD with anxiety, subjects with a past or present comorbid anxiety disorder were allowed to participate (see Table S2, available online, for a summary of the comorbidities in the MDD group). At the time of scanning, all MDD subjects were fully symptomatic and medication naïve.

The computerized Diagnostic Interview Schedule for Children 4.0[48] and the Diagnostic Predictive Scale[49] was used to screen for the presence of any Axis I diagnoses in the HCL adolescents.

In addition to completing forms on basic demographics and general medical and developmental history, all subjects completed the following within three days of their scan session: Edinburgh Handedness Inventory[50], Customary Drinking and Drug Use Record,[51] Family Interview for Genetics Studies,[52] Tanner Stage,[53] Wechsler Abbreviated Scale of Intelligence (WASI),[54] Beck Depression Inventory–II (BDI-II),[55] Children's Depression Rating Scale-Revised (CDRS-R),[56] Children's Global Assessment Scale (CGAS),[57] and Multidimensional Anxiety Scale for Children (MASC).[58] With the exception of the CDRS-R and CGAS, all other measures were self-report. One subject (HCL) failed to provide information for the MASC and was therefore not included in any statistical analyses involving this measure. Given the high proportion of participants in the study whose first language was not English, we measured IQ solely on the basis of the performance measure of the WASI.

Exclusionary criteria for the adolescents with MDD included the following:

1. A CDRS-R *t*-score lower than 55

2. Inability to fully understand and cooperate with the study procedures

3. Having a performance IQ of less than 75

4. Any contraindication to MR imaging (e.g., pregnancy, claustrophobia, ferrometallic implants)

5. Any history of neurological disorders (e.g., head trauma, seizures)

6. A learning disability

7. Prior or present use of antidepressants

8. Any evidence of illicit drug use, misuse of prescription drugs, or more than 2 alcohol drinks per week currently or within the previous month

9. Pre-pubertal status (Tanner stage 1 or 2)

10. Left-handedness

HCL adolescents were excluded from the study for any of the exclusionary criteria for the MDD group, as well as any current or lifetime Axis I psychiatric disorder, any family history of mood or psychotic disorders in first- or second-degree relatives, or a CDRS-R *t*-score higher than 54.

Image Acquisition

All scanning was carried out on a General Electric Discovery MR750 3T scanner (Milwaukee, WI) at the University of California–San Diego. All subjects were instructed to relax and remain awake but motionless during scanning. A fixation cross was displayed on a large screen that was viewed through a small, angled mirror; however, no eye tracking was recorded. Subjects were monitored by video and reminded before the start of the experimental session and in between each scan to remain as still as possible.

The mechanism used in standard PCASL scans to magnetically tag arterial blood is accomplished by applying a series of radiofrequency (RF) pulses and slice selective gradients.[41] However, when there is a mismatch between the phase of successive RF pulses and the phase evolution of flowing spins in the blood (known as the *phase tracking error*), the efficiency of this tagging process can greatly deteriorate, which in turn can lead to highly inaccurate estimates of CBF.[59–60] Thus, we used a series of prescans to measure and minimize the phase tracking error so that the baseline ASL data could be acquired with optimal tagging efficiency and hence, a more precise measurement of CBF.[39] The technical details of this PCASL method are beyond the scope of the current paper and are published elsewhere.[39] The following is a brief summary of the MRI acquisition steps in sequential order (see also Figure 1): Time of flight (TOF) angiographic images were acquired (22cm field of view [FOV], 512×512 matrix, repetition time [TR]=20ms, time to echo [TE]=3.17ms, flip angle=15°, 52 1mm axial slices with an in-plane resolution of 1×1mm, scan time=1:43 min) before manually defining an optimal plane for labeling blood flowing through the feeding arteries (Figure 1A). The coordinates of the tagging plane and the feeding arteries (specifically, the right carotid artery, left carotid artery, and vertebral artery) were saved into a configuration file. The coordinates of the tagging plane were used for setting the tagging plane in all subsequent ASL scans, while the coordinates for the feeding arteries were used by the vessel-encoded ASL scan (described next) for spatial vessel encoding. The second pre-scan employed vessel-encoded ASL[61–63] (TR=3200ms, TE=3.17ms, flip angle=90°, tag duration=2000ms, post labeling delay=400ms, scan time=1:36min) and used the spatial coordinates of the feeding arteries to generate regional masks of the vascular territories (Figure 1B). The final pre-scans involved up to 2 multiphase PCASL (MP-PCASL; TR=3200ms, TE=3.17ms, flip angle=90°, tag duration=2000ms, post labeling delay=400ms, scan time=1:40min) scans using 8 radio frequency phase offsets to estimate the phase tracking errors in each of the arterial territory masks acquired from the previous vascular territory imaging scan (Figure 1C).[59–60] Note

that the first MP-PCASL scan was used to measure the uncorrected phase errors while the second MP-PCASL scan was to verify that the errors were minimized after modulating the RF phase and in-plane gradients to the PCASL pulse train. If the phase tracking errors from the first MP-PCASL scan were less than 20°, then the second MP-PCASL scan was skipped, as modifications to the PCASL pulse train were not needed (Figure 1C). The optimized global RF phase and in-plane gradients determined by the MP-PCASL scan(s) were then applied to the tagging module for the PCASL scan (single-shot spiral readout, TR=4100ms, TE=3.17ms, flip angle=90°, tag duration=2000ms, post labeling delay=1600ms, 30 tagged and 30 control image pairs for 60 volumes total, scan time=4:00min). Thus, the optimized PCASL scan was a conventional PCASL scan, but with added RF phase and gradient specifications (Figure 1D). Afterward, a 36-s scan (TR=4000ms, TE=3.4ms, NEX=9, with 90° excitation pulse turned off for the first 8 repetitions) was acquired to obtain the equilibrium magnetization of cerebrospinal fluid (CSF).[39] A 32-s minimum contrast scan (TR=2000ms, TE=11ms, NEX=2) using an 8-shot spiral acquisition was also acquired to estimate the combined transmit and receive coil inhomogeneities.[64–66] Finally, to correct for blurring in spiral images due to off-resonance fields, a B_0 field map was acquired (TR=500ms, TE1=6.5ms, TE2=8.5ms, flip angle=45°, scan time=1:16min). The acquired field map was then used for offline reconstruction of all ASL data using a *k*-space based fast iterative image reconstruction algorithm.[67] All images, except the TOF and T1-weighted data, were acquired at the same resolution: 24 cm FOV, 64×64 matrix, 20 axial slices 5mm thick with an in-plane resolution of 3.75×3.75mm.

A fast spoiled gradient recalled (FSPGR) sequence was used to collect T1-weighted images: 25.6cm FOV, 256×256 matrix, TR=8.1ms, TE=3.17ms, TI=450ms, flip angle=12°, 168 sagittal slices 1 mm thick with an in-plane resolution of 1×1mm, scan time=8:44 min.

Image Processing and Analysis

All image processing and analyses were conducted with the Analysis of Functional NeuroImages (AFNI) software,[68] FMRIB Software Library (FSL),[69] and Matlab (version 7.10; Natwick, MA). An in-house automated Matlab script utilizing AFNI and FSL tools was used to apply skull-stripping, motion correction, and slice-time correction to the images.[39] For each participant, all ASL images were coregistered to the first volume. Next, the average running difference between the tagged and control images was computed via surround subtraction (i.e., the difference between an image and the average of its 2 nearest neighbors) to yield a perfusion-weighted time series).[70] These uncorrected perfusion data in MR signal intensity units were then converted to calibrated CBF units (milliliters of blood/ 100 grams of tissue per minute) using an estimate of equilibrium magnetization of CSF as a reference signal from the 36-s CSF scan (see Image Acquisition above).[71] The perfusion images were also corrected for transmit/receive coil inhomogeneities by dividing the time series by the minimum contrast image obtained from the 32-s minimum contrast scan (see Image Acquisition above).[64] The time series was then averaged over time to yield a mean CBF value for each voxel. The anatomical images were then aligned to the CBF data and spatially normalized to Talairach[72] standard space in a template provided by AFNI. The matrix derived from transforming the structural images into standard space was then applied to the CBF data, which was subsequently resampled to 4×4×4 mm resolution. Any spurious negative values in the voxels were replaced with zero.[65,73] Finally, a 4.0 mm full-width half-maximum (FWHM) isotropic Gaussian filter was applied to all the voxels.[65,73]

Whole Brain Analysis

Regions of significant group differences (MDD versus HCL) were determined by performing a voxelwise 2-sample *t*-test on CBF values. Significant voxels were required to pass a voxelwise statistical threshold of t_{49}=2.02 (*p*=0.05, uncorrected). To control for

multiple comparisons at =0.05, we computed the minimum number of contiguous voxels passing the voxelwise threshold that would result in a clusterwise 5% probability of being due to chance using 10,000 iterations of Monte Carlo simulations based on an average whole brain mask created from all subjects (downsampled to 4×4×4 mm). According to our simulations, the cluster threshold was 20 voxels. For group comparison, mean regional CBF (rCBF) values were extracted from each of the clusters surviving this 20 voxel threshold.

Region-of-Interest Analysis

Since limbic, paralimbic, and striatal regions have shown divergent rCBF differences in adults with depression, we defined *a priori* regions of interest (ROIs) targeting these areas (all bilateral): amygdala, insula, and striatum. These 3 distinct bilateral ROI masks were generated by the AFNI Talairach Daemon atlas.[74] Since anatomical ROIs are often large, such that the truly active voxels make up a relatively small proportion of any anatomical ROI, we employed Monte Carlo simulations to correct for familywise error rates for each ROI mask separately.[75] Such clusterwise inference methods possess more power compared to methods that adjust false positive probabilities per voxel, while still capturing the spatial nature of fMRI signals and suffering from less multiplicity than voxelwise analyses.[75,76] Regions of significant group differences (MDD versus HCL) within each ROI were determined by performing a voxelwise 2-sample *t*-test on CBF values. To correct for the number of ROIs, a Bonferroni correction was applied at the voxelwise level, such that significant voxels were required to pass a statistical threshold of $t_{49}=2.51$ ($p<0.0167$, corrected). Thus, the cluster threshold was determined via Monte Carlo simulations that together with the voxelwise threshold resulted in an overall 5% probability of a significant cluster surviving due to chance across all three ROIs. According to our simulations, the cluster thresholds were 3, 5, and 4 voxels for the amygdala, insula, and striatum, respectively. For group comparison, mean rCBF values were extracted from each of the clusters that survived each respective ROI's cluster threshold.

Linear Mixed Effects Model With Anxiety as a Covariate

Additionally, we ran a linear mixed effects model with rCBF as the within-subjects factor (fixed effect), group (MDD v. HCL) as the between-subjects factor, participant as the random effect, and a comorbid diagnosis of an anxiety disorder as a dichotomous covariate. Significant voxels were required to pass a voxelwise statistical threshold of $F_{1,48}=4.04$ ($p=0.05$, uncorrected). For group comparison, mean rCBF values were extracted from each of the clusters that survived the whole brain cluster threshold of 20 voxels (see Whole Brain Analysis, above).

Sociodemographic and Clinical Scales Analysis

Statistical analyses of all demographic and clinical scales were computed with R[77] and Matlab (version 7.10; Natwick, MA). Within the MDD group only, correlations between extracted mean rCBF values in the surviving clusters identified in the whole brain and ROI analyses and clinical data (i.e., BDI-II, CDRS-R, CGAS, MASC, age of onset, duration of illness, and number of depressive episodes) were examined using 2-tailed tests of Spearman's rank correlation coefficient (r_s).

Results

Sociodemographic and Clinical Scales

The MDD and HCL groups did not significantly differ in age ($t_{49}=1.22$, $p=0.22$), gender ($\chi^2_1=0.007$, $p=0.93$), ethnicity ($U=338$, $p=0.81$), Tanner stage ($U=322$, $p=0.96$), performance IQ ($t_{49}=1.20$ $p=0.23$), or socioeconomic status ($U=252.5$, $p=0.17$). MDD

adolescents showed significantly greater levels of depression as measured by BDI-II (t_{49}=10.7, p<0.001) and CDRS-R (t_{49}=39.6, p<0.001), significantly greater levels of anxiety as measured by MASC (t_{48}=6.87, p<0.001), as well as significantly lower assessment of general function as measured by CGAS compared with their HCL counterparts (U=622, p<0.001). MASC scores between adolescents with and without comorbid anxiety disorders did not differ significantly (t_{23}=0.83, p>0.05). For more details, see Table S1, available online.

Whole Brain Analysis

Twelve regions survived the analysis correcting for multiple comparisons (see Whole Brain Analysis under Method). Eight regions revealed significantly lower mean rCBF in the MDD compared to the HCL group: bilateral parahippocampal gyri/insula, right inferior frontal gyrus (IFG)/dorsolateral prefrontal cortex (DLPFC), right anterior cingulate cortex (ACC), right middle occipital gyrus, left inferior temporal gyrus, and bilateral cerebellum (see Table 1 and Figure 2). Four regions revealed significantly higher mean rCBF in the MDD compared to HCL group: right subcallosal cingulate, right putamen/lentiform nucleus (extending rostrally into the insula), and bilateral fusiform gyrus (see Table 1 and Figure 2).

Region-of-Interest Analysis

Five regions survived the analysis correcting for multiple comparisons (see Region-of-Interest Analysis under Method). Three regions revealed significantly lower mean rCBF in the MDD compared to the HCL group: right amygdala, and bilateral inferior insula (see Table 2 and Figure 3). Two regions revealed significantly higher mean rCBF in the MDD compared to the HCL group: right superior insula (BA13) and right putamen/lentiform nucleus (see Table 2 and Figure 3).

Linear Mixed Effects Model With Anxiety as a Covariate

Seven regions survived the analysis correcting for multiple comparisons (see Whole Brain Analysis under Method). Six regions revealed significantly lower mean rCBF in the MDD compared to the HCL group: right inferior frontal gyrus, right anterior cingulate cortex, right cerebellum, left insula, right cingulate gyrus, and left middle temporal gyrus (see Table S3, available online). One region revealed significantly higher mean rCBF in the MDD compared to the HCL group: right putamen/lentiform nucleus (see Table S3, available online). Five of these clusters overlapped with the whole brain results (see Figure S1, available online): right IFG/DLPFC (73 overlapping voxels), right ACC (40 overlapping voxels), left insula (22 overlapping voxels), right putamen/lentiform nucleus (18 overlapping voxels), and right cerebellum (16 overlapping voxels). The directionality of perfusion differences between MDD and HCL within these clusters exactly matched the directionality of perfusion differences between MD and HCL in analogous clusters in the whole brain analysis, thereby suggesting that anxiety did not drive the differences found in our main findings.

Correlations Between rCBF and Clinical Characteristics (All Subjects With MDD)

No significant correlations were found between the clinical data and mean rCBF from the 12 clusters resulting from the whole brain analysis or the 5 clusters resulting from the ROI analysis (all p>0.05).

Correlations Between rCBF and Clinical Characteristics (Only Subjects With MDD Without Comorbidities)

Correlational analyses were also run among the MDD subjects without any comorbid diagnoses (n=12). Both mean rCBF of the left parahippocampal gyrus/insula and mean

rCBF of the right IFG/DLPFC from the whole brain analysis correlated positively with age of onset (r_s=0.683, p=0.02 and r_s=0.619, p=0.042, respectively). Mean rCBF of the left insula from the ROI analysis correlated both positively with age of onset (r_s=0.762, p=0.006;) and negatively with duration of depression (r_s=−0.652, p=0.03). Finally, mean rCBF of the right inferior insula from the ROI analysis correlated negatively with the number of depressive episodes (r_s=−0.724, p=0.011).

Discussion

In the present study, we employed a novel method of PCASLwith optimized tagging efficiency[39] on a large cohort of nonmedicated adolescents with MDD and well-matched HCL adolescents in order to assess baseline rCBF differences between these two groups. Our study yielded 2 main results. First, we observed significant hypoperfusion in the MDD relative to the HCL group within frontal, amygdalar, insular, cingular, and cerebellar regions. Second, we found significant hyperperfusion in the MDD compared to the HCL adolescents within the subcallosal cingulate, putamen, and fusiform gyri. Importantly, these results did not qualitatively change even when we controlled for comorbid anxiety disorders in our brain analyses (see Results for more details).

In our leading hypothesis, we predicted finding rCBF differences in frontal, limbic, paralimbic, cingulate, and striatal areas. More specifically, we predicted lower rCBF in the MDD group among frontal regions. Indeed, we observed hypoperfusion in the inferior frontal gyrus and dorsolateral prefrontal cortex (see Table 1 and Figure 2) in the MDD relative to HCL adolescents. These findings mirror previous PET,[5–9,78–83] SPECT,[84–85] ASL[33–36] work showing lower baseline frontal rCBF, as well as resting state BOLD[86,87] data showing altered functional connectivity in dorsolateral prefrontal cortex at both rest[86] and during a cognitive task[87] in adults with MDD. Hypoactivity in frontal and prefrontal areas has been strongly linked not only to psychomotor retardation,[80–83] but also to impaired executive functioning (e.g., attention, working memory, and decision making).[88–89] Together with these studies, our results suggest that reduced perfusion in these regions may be associated with some of the cognitive and motor symptoms found in adolescent MDD.

As hypothesized, we also found rCBF differences in limbic, paralimbic, and cingulate areas between MDD and HCL adolescents (see Tables 1–2 and Figures 2–3). Our finding of hypoperfusion in the anterior cingulate cortex of adolescents with MDD is consistent with several perfusion[34–36, 81,84–85, 90–], metabolism[91], and resting state BOLD[15] studies of adult depression. On the other hand, our observation of hypoperfusion in the amygdala and insula is in partial contrast with some of the prior adult perfusion[33,35] showing hyperperfusion in these areas, as well as resting state BOLD studies on adult[92–95,15] and adolescent[42–96] depression failing to show altered connectivity differences. The disparity in our results may be due to differences in patient sample (e.g., age, medication status, comorbidities) or imaging technique (PCASL with optimized tagging efficiency). Nevertheless, the anterior cingulate cortex, amygdala, and insula have been shown to be involved in the processing of emotion and motivation;[97–32] thus, dysfunction in these structures may underlie some of the core affective symptoms seen in major depressive disorder.[92–94,15] It is therefore possible that our observation of hypoperfusion in these affective processing regions is a reflection of reduced motivation or feelings of anhedonia that are commonly present in adolescent depression.

Consistent with our second hypothesis, we also found significant hyperperfusion in the MDD relative to HCL group in the right subcallosal cingulate and right superior insula (see Tables 1–2 and Figures 2–3). Our results in the subcallosal cingulate are substantiated by the current literature of adults with depression exhibiting hyperperfusion in this region during

baseline,[7,32] as well as our previously published neuroimaging work on greater task-evoked activation in this region among adolescents with depression.[100] Given its anatomical connections to frontal, limbic, and paralimbic structures,[101] the subcallosal cingulate is thought to lie at the interface of cognitive and affective processing, such that aberrant functioning in this region leads to impaired emotion regulation.[7,28] Indeed, several perfusion studies in adult MDD have demonstrated elevated baseline rCBF in the subcallosal cingulate during depressive relapse[102–103] that decreases with remission,[104] effective antidepressant treatment,[105–106] electroconvulsive therapy,[107] and deep brain stimulation.[29, 108,109] Reduced glucose metabolism in the insula has also been shown to correlate with symptom improvement among adults with treatment-resistant MDD,[30] while increased insular activation has been reported in both healthy adults[110–112] and adults with depression[113] while experiencing exceptionally negative emotions. Similarly, BOLD rsfMRI studies in both young adults[17,21] and adolescents[21–23] have shown altered functional connectivity in affective networks based within the subcallosal cingular area, particularly between paralimbic and limbic sites, including the insula, amygdala, and striatal structures. One possible interpretation of our results is that atypical hyperactivity in the subcallosal cingulate and superior insula leads to overreaction to and improper emotional regulation of negative stimuli during adolescent depression. However, more studies are needed to investigate how both hypo- and hyperperfusion within distinct parts of the insula relate to both adolescent and adult MDD.

Abnormally increased metabolism in the putamen and fusiform gyri in adult depression has been less frequently described.[35,114,115] However, some evidence for the role of these regions in affective processing in adult depression exists, including the involvement of the putamen in the processing of negatively valenced stimuli[112] and an observed increase in putaminal rCBF during acute depression[34] that decreases with remission.[102] More recently, one resting state BOLD study reported weaker functional connectivity between the ventral putamen and ventromedial prefrontal cortex in adults with MDD.[16] Task-based fMRI studies have also documented increased activation in the putamen in adult healthy controls,[115–117] as well as increased activation in the fusiform gyrus in adults with depression[113] and control[115–117] adults during viewing emotional stimuli. Similar to the current study, increased rCBF has also been observed in the fusiform gyrus of adults with depression at rest[114]. These results suggest that future work should investigate whether the putamen and fusiform are critical to adverse responses to negative stimuli in adolescents with depression and whether these regions are functionally connected to other structures involved in affective processing.[118]

Lastly, our observation of cerebellar hypoperfusion in adolescents with MDD is consistent with emerging evidence that the cerebellum influences not only motor function, but also affective processing via connections to limbic structures.[119–123] Cerebellar lesions in both adults[124] and children[125] lead to psychomotor retardation, passivity, and a blunting of emotion that is behaviorally similar to depression and other mood disorders. PET data in adults with depression have also shown decreased cerebellar rCBF and lower brain activation at baseline.[126] Likewise, resting state BOLD fMRI[127–130] has demonstrated altered cerebellar functional connectivity with parts of prefrontal cortex,[127–130] cingulate cortex,[129,130] temporal poles,[129,130] and the fusiform gyrus.[128,130] While more studies are needed to clarify the role of the cerebellum in major depression and mood disorders, our current results suggest that there are significant cerebellar differences between adolescents with MDD and healthy controls.

Along with several other perfusion studies on adult depression,[33–36,131] we did not find any significant correlations between mean rCBF and clinical data among our MDD group. When omitting MDD subjects with a comorbid anxiety disorder from our correlational analyses,

however, we did find some significant associations between mean rCBF and clinical characteristics (see Results for more details). Although these results do seem to suggest that our study and prior studies[33–36,131] may not have found predictive relationships between mean rCBF and clinical data due to the homogeneity of MDD patients recruited, given the low number of subjects (n=12) and the total number of correlation tests run (7) performed for this analysis, these results must be viewed with caution.

Our results must nevertheless be interpreted in light of the study's limitations. As the present study is cross-sectional, we cannot address whether these perfusion patterns precede or are a product of adolescent depression. Future longitudinal studies are therefore needed to examine cerebral blood flow levels prior to the onset of adolescent depression and how they may normalize with recovery. Task-based studies could also be carried out in order to assess how perfusion patterns among these executive, affective, and motor networks differ between adolescents with depression and healthy controls when faced with emotional stimuli and/or cognitive tasks and to assess to what degree, if any, these perfusion patterns change. Correlating changes in regional CBF with performance on cognitive testing (particularly in the domains of memory, affect, and psychomotor function) outside of the scanner may also further elucidate how differences in these brain networks may be related to the clinical symptoms of adolescents with MDD. Functional connectivity analyses with perfusion data would also be immensely useful in ascertaining the distributed brain network that is affected by adolescent depression. Furthermore, longitudinal studies could assess how the strength of these network connections change in terms of blood flow during the progression of MDD. It should be noted that the optimized PCASL scan sequence presented in this paper was not long enough (4 minutes) for us to perform a functional connectivity analysis or examine time effects (beginning versus end of scan), as more acquisitions would have been needed to ensure adequate signal-to-noise ratio (SNR). In comparison to BOLD resting state fMRI, ASL perfusion imaging tends to yield lower SNR and necessitates a pair of volumes (tagged v. control) to produce a single CBF-weighted volume, hence requiring longer scan times.[132,133] Despite these methodological limitations, the optimized tagging efficiency of our PCASL method yields high quality CBF images and establishes the use of a novel ASL-based method to noninvasively study perfusion in adolescent depression. Future studies could test our novel optimized PCASL method with a longer scan sequence in order to investigate functional connectivity differences between adolescents with depression and healthy adolescents (see Chuang *et al.*, 2008,[134] Viviani *et al.*, 2011,[133] and Liu *et al.*, 2013[135] for recent examples of functional connectivity analyses on pulsed and continuous ASL perfusion data using much longer scan times in adults). Finally, the absence of a comparator morbid group (e.g., anxiety disorders) in the present study restricts how much our findings can be generalized to adolescents with depression without comorbidities. While our voxel-based analyses controlling for comorbid anxiety suggest that anxiety did not contribute significantly to our brain results, future studies must nevertheless include comparator morbid groups to validate and replicate our observations.

The clinical implications of our findings suggest that patterns of baseline regional CBF within the fronto-limbic-cingulate-striatal-cerebellar network may be a candidate biomarker for adolescent MDD. Determining whether and how divergence of these rCBF patterns from that typical of healthy adolescents relates to depressive severity and other clinical characteristics of adolescent MDD could potentially assist in the early diagnosis, intervention, and potential prevention of this disorder. Additionally, since several antidepressants affect blood flow,[37,38] rCBF could also be utilized to help determine potential therapeutic targets for treatment and to assess pharmacological effects.[105,106,136] Nevertheless, more research is needed to specifically link identifying patterns of perfusion with the clinical symptoms and behaviors that characterize adolescent MDD.

Our results establish the use of advanced ASL methods as a highly effective noninvasive neuroimaging tool for measuring baseline CBF in both adolescents with depression and healthy adolescents. Compared to techniques such as PET or SPECT, ASL enjoys the practical advantages of being noninvasive, is relatively straightforward to implement, and allows for repeated scanning safely within a single subject without the use of radioisotopes. BOLD fMRI is also noninvasive, but offers information that is subtly distinct from ASL: functional connectivity analyses of BOLD resting state data can be used to identify intrinsic networks in the brain, while ASL is able to show the base utilization of these individual network components (i.e., brain regions) by measuring actual blood flow. Interestingly, at least one study has shown no correlation between functional connectivity and mean perfusion levels, suggesting that both of these aspects of the resting state could potentially represent different brain markers.[133] However, the BOLD signal is not an absolute measure of brain function and is sensitive to vascular factors such as blood flow. Thus, the estimate of an absolute neurophysiological brain measure from ASL offers great promise as a noninvasive technique for detecting subtle changes in brain function for the purposes of diagnosis and treatment assessment in clinical research studies, particularly when used in conjunction with BOLD fMRI techniques.[13,137] Relative to other ASL methods, PCASL has a higher test–retest reliability,[138] higher intrasubject SNR,[40] and lower intersubject variability[139] and consequently, has become progressively more popular among researchers wishing to noninvasively measure cerebral blood flow.[11,109] Thus, as PCASL methods become more refined and widely available, their potential for clinical utility will continue to grow.

In conclusion, we used a novel method of pseudocontinuous arterial spin labeling that optimizes tagging efficiency and found abnormal hypoperfusion in executive, affective, and motor networks of the brain and abnormal hyperperfusion in areas supporting emotional regulation in a relatively large sample of medication-naïve adolescents with depression compared to a group of well-matched healthy controls. Combined with prior neuroimaging work on depression, our results suggest that dysfunction in these networks may contribute to the cognitive, affective, and psychomotor symptoms commonly present in adolescent depression. Finally, our study demonstrates the efficacy of pseudocontinuous arterial spin labeling in understanding adolescent major depressive disorder and advances the possibility of using such arterial spin labeling methods for clinical purposes in the future.

Supplementary Material

Refer to Web version on PubMed Central for supplementary material.

Acknowledgments

References

1. The World Health Organization. The global burden of disease: 2004 update, Table 9: Estimated prevalence of moderate and severe disability for leading disabling conditions by age, for high-income and low- and middle-income countries, 2004. 2008. http://www.who.int/healthinfo/global_burden_disease/GBD_report2004update_full.pdf

2. Kessler RC, Berglund P, Demler O, et al. The epidemiology of major depressive disorder: results from the National Comorbidity Survey Replication (NCS-R). JAMA : the journal of the American Medical Association. Jun 18; 2003 289(23):3095–3105. [PubMed: 12813115]

3. Kessler RC, Angermeyer M, Anthony JC, et al. Lifetime prevalence and age-of-onset distributions of mental disorders in the World Health Organization's World Mental Health Survey Initiative. World psychiatry : official journal of the World Psychiatric Association (WPA). Oct; 2007 6(3): 168–176. [PubMed: 18188442]

4. Pine DS, Cohen E, Cohen P, Brook J. Adolescent depressive symptoms as predictors of adult depression: moodiness or mood disorder? The American journal of psychiatry. Jan; 1999 156(1): 133–135. [PubMed: 9892310]

5. Davidson RJ, Pizzagalli D, Nitschke JB, Putnam K. Depression: perspectives from affective neuroscience. Annual review of psychology. 2002; 53:545–574.

6. Mayberg HS. Modulating dysfunctional limbic-cortical circuits in depression: towards development of brain-based algorithms for diagnosis and optimised treatment. British medical bulletin. 2003; 65:193–207. [PubMed: 12697626]

7. Seminowicz DA, Mayberg HS, McIntosh AR, et al. Limbic-frontal circuitry in major depression: a path modeling metanalysis. NeuroImage. May; 2004 22(1):409–418. [PubMed: 15110034]

8. Videbech P. PET measurements of brain glucose metabolism and blood flow in major depressive disorder: a critical review. Acta psychiatrica Scandinavica. Jan; 2000 101(1):11–20. [PubMed: 10674946]

9. Smith DJ, Cavanagh JT. The use of single photon emission computed tomography in depressive disorders. Nuclear medicine communications. Mar; 2005 26(3):197–203. [PubMed: 15722900]

10. Detre JA, Wang J. Technical aspects and utility of fMRI using BOLD and ASL. Clinical neurophysiology : official journal of the International Federation of Clinical Neurophysiology. May; 2002 113(5):621–634. [PubMed: 11976042]

11. Detre JA, Wang J, Wang Z, Rao H. Arterial spin-labeled perfusion MRI in basic and clinical neuroscience. Current opinion in neurology. Aug; 2009 22(4):348–355. [PubMed: 19491678]

12. Greicius M. Resting-state functional connectivity in neuropsychiatric disorders. Current opinion in neurology. Aug; 2008 21(4):424–430. [PubMed: 18607202]

13. Brown GGC C, Liu TT. Measurement of cerebral perfusion with arterial spin labeling: Part 2. Applications. J Int Psychol Soc. 2007; 23:526–538.

14. Fox MD, Raichle ME. Spontaneous fluctuations in brain activity observed with functional magnetic resonance imaging. Nature reviews Neuroscience. Sep; 2007 8(9):700–711.

15. Anand A, Li Y, Wang Y, Lowe MJ, Dzemidzic M. Resting state corticolimbic connectivity abnormalities in unmedicated bipolar disorder and unipolar depression. Psychiatry research. Mar 31; 2009 171(3):189–198. [PubMed: 19230623]

16. Furman DJ, Hamilton JP, Gotlib IH. Frontostriatal functional connectivity in major depressive disorder. Biology of mood and anxiety disorders. 2011; 1(1):11. [PubMed: 22737995]

17. Greicius MD, Flores BH, Menon V, et al. Resting-state functional connectivity in major depression: abnormally increased contributions from subgenual cingulate cortex and thalamus. Biological psychiatry. Sep 1; 2007 62(5):429–437. [PubMed: 17210143]

18. Hamilton JP, Chen G, Thomason ME, Schwartz ME, Gotlib IH. Investigating neural primacy in Major Depressive Disorder: multivariate Granger causality analysis of resting-state fMRI time-series data. Molecular psychiatry. Jul; 2011 16(7):763–772. [PubMed: 20479758]

19. Sheline, YI.; Price, JL.; Yan, Z.; Mintun, MA. Resting-state functional MRI in depression unmasks increased connectivity between networks via the dorsal nexus; Proceedings of the National Academy of Sciences of the United States of America; Jun 15 2010; p. 11020-11025.

20. Veer IM, Beckmann CF, van Tol MJ, et al. Whole brain resting-state analysis reveals decreased functional connectivity in major depression. Frontiers in systems neuroscience. 2010; 4

21. Davey CG, Harrison BJ, Yucel M, Allen NB. Regionally specific alterations in functional connectivity of the anterior cingulate cortex in major depressive disorder. Psychological medicine. Oct; 2012 42(10):2071–2081.

22. Connolly C, W J, Ho TC, Hoeft F, Wolkowitz O, Eisendrath S, Frank G, Hendren R, Max JE, Paulus MP, Tapert SF, Banerjee D, Simmons AN, Yang TT. Resting state functional connectivity of subgenual anterior cingulate cortex in adolescents with depression. Biological psychiatry. under review.

23. Cullen KR, Gee DG, Klimes-Dougan B, et al. A preliminary study of functional connectivity in comorbid adolescent depression. Neuroscience letters. Sep 4; 2009 460(3):227–231. [PubMed: 19446602]

24. Liu Z, Xu C, Xu Y, et al. Decreased regional homogeneity in insula and cerebellum: a resting-state fMRI study in patients with major depression and subjects at high risk for major depression. Psychiatry research. Jun 30; 2010 182(3):211–215. [PubMed: 20493670]

25. Bokkers RP, Bremmer JP, van Berckel BN, et al. Arterial spin labeling perfusion MRI at multiple delay times: a correlative study with H(2)(15)O positron emission tomography in patients with symptomatic carotid artery occlusion. Journal of cerebral blood flow and metabolism : official journal of the International Society of Cerebral Blood Flow and Metabolism. Jan; 2010 30(1):222–229. [PubMed: 19809464]

26. Borogovac A, Asllani I. Arterial Spin Labeling (ASL) fMRI: advantages, theoretical constrains, and experimental challenges in neurosciences. International journal of biomedical imaging. 2012; 2012:818456. [PubMed: 22966219]

27. Bonne O, Krausz Y. Pathophysiological significance of cerebral perfusion abnormalities in major depression-trait or state marker? European neuropsychopharmacology : the journal of the European College of Neuropsychopharmacology. Aug; 1997 7(3):225–233. [PubMed: 9213083]

28. Mayberg HS. Limbic-cortical dysregulation: a proposed model of depression. The Journal of neuropsychiatry and clinical neurosciences. Summer;1997 9(3):471–481. [PubMed: 9276848]

29. Mayberg HS, Lozano AM, Voon V, et al. Deep brain stimulation for treatment-resistant depression. Neuron. Mar 3; 2005 45(5):651–660. [PubMed: 15748841]

30. Lozano AM, Mayberg HS, Giacobbe P, Hamani C, Craddock RC, Kennedy SH. Subcallosal cingulate gyrus deep brain stimulation for treatment-resistant depression. Biological psychiatry. Sep 15; 2008 64(6):461–467. [PubMed: 18639234]

31. Holtzheimer PE 3rd, Mayberg HS. Deep brain stimulation for treatment-resistant depression. The American journal of psychiatry. Dec; 2010 167(12):1437–1444. [PubMed: 21131410]

32. Pizzagalli DA. Frontocingulate dysfunction in depression: toward biomarkers of treatment response. Neuropsychopharmacology : official publication of the American College of Neuropsychopharmacology. Jan; 2011 36(1):183–206. [PubMed: 20861828]

33. Clark CP, Brown GG, Archibald SL, et al. Does amygdalar perfusion correlate with antidepressant response to partial sleep deprivation in major depression? Psychiatry research. Jan 30; 2006 146(1):43–51. [PubMed: 16380239]

34. Lui S, Parkes LM, Huang X, et al. Depressive disorders: focally altered cerebral perfusion measured with arterial spin-labeling MR imaging. Radiology. May; 2009 251(2):476–484. [PubMed: 19401575]

35. Duhameau B, Ferre JC, Jannin P, et al. Chronic and treatment-resistant depression: a study using arterial spin labeling perfusion MRI at 3Tesla. Psychiatry research. May 30; 2010 182(2):111–116. [PubMed: 20427157]

36. Jarnum H, Eskildsen SF, Steffensen EG, et al. Longitudinal MRI study of cortical thickness, perfusion, and metabolite levels in major depressive disorder. Acta psychiatrica Scandinavica. Dec; 2011 124(6):435–446. [PubMed: 21923809]

37. Viviani R, Abler B, Seeringer A, Stingl JC. Effect of paroxetine and bupropion on human resting brain perfusion: an arterial spin labeling study. NeuroImage. Jul 16; 2012 61(4):773–779. [PubMed: 22446490]

38. Noskin O, Jafarimojarrad E, Libman RB, Nelson JL. Diffuse cerebral vasoconstriction (Call-Fleming syndrome) and stroke associated with antidepressants. Neurology. Jul 11; 2006 67(1):159–160. [PubMed: 16832100]

39. Shin DD, Liu TT, Wong EC, Shankaranarayanan A, Jung Y. Pseudocontinuous arterial spin labeling with optimized tagging efficiency. Magnetic resonance in medicine : official journal of the Society of Magnetic Resonance in Medicine / Society of Magnetic Resonance in Medicine. Oct; 2012 68(4):1135–1144. [PubMed: 22234782]

40. Wu WC, Fernandez-Seara M, Detre JA, Wehrli FW, Wang J. A theoretical and experimental investigation of the tagging efficiency of pseudocontinuous arterial spin labeling. Magnetic resonance in medicine : official journal of the Society of Magnetic Resonance in Medicine / Society of Magnetic Resonance in Medicine. Nov; 2007 58(5):1020–1027. [PubMed: 17969096]

41. Dai W, Garcia D, de Bazelaire C, Alsop DC. Continuous flow-driven inversion for arterial spin labeling using pulsed radio frequency and gradient fields. Magnetic resonance in medicine : official journal of the Society of Magnetic Resonance in Medicine / Society of Magnetic Resonance in Medicine. Dec; 2008 60(6):1488–1497. [PubMed: 19025913]

42. Yang TT, Simmons AN, Matthews SC, et al. Adolescents with major depression demonstrate increased amygdala activation. Journal of the American Academy of Child and Adolescent Psychiatry. Jan; 2010 49(1):42–51. [PubMed: 20215925]

43. Sliz D, Hayley S. Major depressive disorder and alterations in insular cortical activity: a review of current functional magnetic imaging research. Frontiers in human neuroscience. 2012; 6:323. [PubMed: 23227005]

44. Forbes EE, Hariri AR, Martin SL, et al. Altered striatal activation predicting real-world positive affect in adolescent major depressive disorder. The American journal of psychiatry. Jan; 2009 166(1):64–73. [PubMed: 19047324]

45. Forbes EE. fMRI studies of reward processing in adolescent depression. Neuropsychopharmacology : official publication of the American College of Neuropsychopharmacology. Jan; 2011 36(1):372–373. [PubMed: 21116265]

46. Kaufman J, Martin A, King RA, Charney D. Are child-, adolescent-, and adult-onset depression one and the same disorder? Biological psychiatry. Jun 15; 2001 49(12):980–1001. [PubMed: 11430841]

47. Kaufman J, Birmaher B, Brent DA, Ryan ND, Rao U. K-SADS-PL. Journal of the American Academy of Child and Adolescent Psychiatry. Oct.2000 39(10):1208. [PubMed: 11026169]

48. Shaffer D, Fisher P, Lucas CP, Dulcan MK, Schwab-Stone ME. NIMH Diagnostic Interview Schedule for Children Version IV (NIMH DISC-IV): description, differences from previous versions, and reliability of some common diagnoses. Journal of the American Academy of Child and Adolescent Psychiatry. Jan; 2000 39(1):28–38. [PubMed: 10638065]

49. Lucas CP, Zhang H, Fisher PW, et al. The DISC Predictive Scales (DPS): efficiently screening for diagnoses. Journal of the American Academy of Child and Adolescent Psychiatry. Apr; 2001 40(4):443–449. [PubMed: 11314570]

50. Oldfield RC. The assessment and analysis of handedness: the Edinburgh inventory. Neuropsychologia. Mar; 1971 9(1):97–113. [PubMed: 5146491]

51. Brown SA, Myers MG, Lippke L, Tapert SF, Stewart DG, Vik PW. Psychometric evaluation of the Customary Drinking and Drug Use Record (CDDR): a measure of adolescent alcohol and drug involvement. Journal of studies on alcohol. Jul; 1998 59(4):427–438. [PubMed: 9647425]

52. Maxwell, ME. Family Interview for Genetic Studies (FIGS): A manual for FIGS. Rockville, MD: National Institute of Mental Health; 1992.

53. Tanner, J. Growth and Adolescence. Oxford: Blackwell; 1962.

54. Wechsler, D. Wechsler Abbreviated Scale of Intelligence Administration and Scoring Manual. San Antonio, TX: The Psychological Corporation; 1999.

55. Beck, AT.; Steer, RA.; Brown, GK. Beck Depression Inventory-Second Edition Manual. San Antonio, TX: The Psychological Corporation; 1996.

56. Poznanski, EO. Children's Depressing Rating Scale-Revised (CDRS-R). Western Psychological Services; 1996.

57. Shaffer D, Gould MS, Brasic J, et al. A children's global assessment scale (CGAS). Archives of general psychiatry. Nov; 1983 40(11):1228–1231. [PubMed: 6639293]

58. March JS, Parker JD, Sullivan K, Stallings P, Conners CK. The Multidimensional Anxiety Scale for Children (MASC): factor structure, reliability, and validity. Journal of the American Academy of Child and Adolescent Psychiatry. Apr; 1997 36(4):554–565. [PubMed: 9100431]

59. Jung Y, Wong EC, Liu TT. Multiphase pseudocontinuous arterial spin labeling (MP-PCASL) for robust quantification of cerebral blood flow. Magnetic resonance in medicine : official journal of the Society of Magnetic Resonance in Medicine / Society of Magnetic Resonance in Medicine. Sep; 2010 64(3):799–810. [PubMed: 20578056]

60. Jung, Y.; Liu, TT. ISMRM. Stockhold, Sweden: 2010. Fast CBF estimation in multi-phase pseudo-continuous arterial spin labeling (MP-PCASL) using signal demodulation.

61. Wong EC. Vessel-encoded arterial spin-labeling using pseudocontinuous tagging. Magnetic resonance in medicine : official journal of the Society of Magnetic Resonance in Medicine / Society of Magnetic Resonance in Medicine. Dec; 2007 58(6):1086–1091. [PubMed: 17969084]

62. Kansagra AP, Wong EC. Mapping of vertebral artery perfusion territories using arterial spin labeling MRI. Journal of magnetic resonance imaging : JMRI. Sep; 2008 28(3):762–766. [PubMed: 18777538]

63. Wong, E.; Kansagra, A. ISMRM. Toronto, Cananda: 2008. Mapping middle cerebral artery branch territories with vessel encoded pseudocontinuous ASL: Sine/Cosine tag modulation and data clustering in tagging efficiency space.

64. Brumm KP, Perthen JE, Liu TT, Haist F, Ayalon L, Love T. An arterial spin labeling investigation of cerebral blood flow deficits in chronic stroke survivors. NeuroImage. Jul 1; 2010 51(3):995–1005. [PubMed: 20211268]

65. Wierenga CE, Dev SI, Shin DD, et al. Effect of mild cognitive impairment and APOE genotype on resting cerebral blood flow and its association with cognition. Journal of cerebral blood flow and metabolism : official journal of the International Society of Cerebral Blood Flow and Metabolism. Aug; 2012 32(8):1589–1599. [PubMed: 22549621]

66. Wang J, Qiu M, Constable RT. In vivo method for correcting transmit/receive nonuniformities with phased array coils. Magnetic resonance in medicine : official journal of the Society of Magnetic Resonance in Medicine / Society of Magnetic Resonance in Medicine. Mar; 2005 53(3):666–674. [PubMed: 15723397]

67. Noll DC, Fessler JA, Sutton BP. Conjugate phase MRI reconstruction with spatially variant sample density correction. IEEE transactions on medical imaging. Mar; 2005 24(3):325–336. [PubMed: 15754983]

68. Cox RW. AFNI: software for analysis and visualization of functional magnetic resonance neuroimages. Computers and biomedical research, an international journal. Jun; 1996 29(3):162–173.

69. Smith SM, Jenkinson M, Woolrich MW, et al. Advances in functional and structural MR image analysis and implementation as FSL. NeuroImage. 2004; 23(1):S208–219. [PubMed: 15501092]

70. Liu TT, Wong EC. A signal processing model for arterial spin labeling functional MRI. NeuroImage. Jan 1; 2005 24(1):207–215. [PubMed: 15588612]

71. Chalela JA, Alsop DC, Gonzalez-Atavales JB, Maldjian JA, Kasner SE, Detre JA. Magnetic resonance perfusion imaging in acute ischemic stroke using continuous arterial spin labeling. Stroke; a journal of cerebral circulation. Mar; 2000 31(3):680–687.

72. Talairach, J.; Tournoux, P. Co-planar Stereotaxis Atlas of the Human Brain. New York: Theime; 1998. Three-Dimensional Proportional System: An Approach to Cerebral Imaging.

73. Brown GG, Eyler Zorrilla LT, Georgy B, Kindermann SS, Wong EC, Buxton RB. BOLD and perfusion response to finger-thumb apposition after acetazolamide administration: differential relationship to global perfusion. Journal of cerebral blood flow and metabolism : official journal of the International Society of Cerebral Blood Flow and Metabolism. Jul; 2003 23(7):829–837. [PubMed: 12843786]

74. Lancaster JL, Woldorff MG, Parsons LM, et al. Automated Talairach atlas labels for functional brain mapping. Human brain mapping. Jul; 2000 10(3):120–131. [PubMed: 10912591]

75. Forman SD, Cohen JD, Fitzgerald M, Eddy WF, Mintun MA, Noll DC. Improved assessment of significant activation in functional magnetic resonance imaging (fMRI): use of a cluster-size threshold. Magnetic resonance in medicine : official journal of the Society of Magnetic Resonance in Medicine / Society of Magnetic Resonance in Medicine. May; 1995 33(5):636–647. [PubMed: 7596267]

76. Nichols TE. Multiple testing corrections, nonparametric methods, and random field theory. NeuroImage. Aug 15; 2012 62(2):811–815. [PubMed: 22521256]

77. R Development Core Team. A Language and Environment for Statistical Computing. 2nd2012. http://cran.r-project.org/docs/manuals/fullrefman.pdf

78. Rogers MA, Bradshaw JL, Pantelis C, Phillips JG. Frontostriatal deficits in unipolar major depression. Brain research bulletin. Nov 1; 1998 47(4):297–310. [PubMed: 9886780]

79. Dolan RJ, Bench CJ, Liddle PF, et al. Dorsolateral prefrontal cortex dysfunction in the major psychoses; symptom or disease specificity? Journal of neurology, neurosurgery, and psychiatry. Dec; 1993 56(12):1290–1294.

80. Galynker, Cai J, Ongseng F, Finestone H, Dutta E, Serseni D. Hypofrontality and negative symptoms in major depressive disorder. Journal of nuclear medicine : official publication, Society of Nuclear Medicine. Apr; 1998 39(4):608–612.

81. Baxter LR Jr, Phelps ME, Mazziotta JC, et al. Cerebral metabolic rates for glucose in mood disorders. Studies with positron emission tomography and fluorodeoxyglucose F 18. Archives of general psychiatry. May; 1985 42(5):441–447. [PubMed: 3872649]

82. Martinot JL, Hardy P, Feline A, et al. Left prefrontal glucose hypometabolism in the depressed state: a confirmation. The American journal of psychiatry. Oct; 1990 147(10):1313–1317. [PubMed: 2399999]

83. Bench CJ, Friston KJ, Brown RG, Scott LC, Frackowiak RS, Dolan RJ. The anatomy of melancholia--focal abnormalities of cerebral blood flow in major depression. Psychological medicine. Aug; 1992 22(3):607–615. [PubMed: 1410086]

84. Pagani M, Gardner A, Salmaso D, et al. Principal component and volume of interest analyses in depressed patients imaged by 99mTc-HMPAO SPET: a methodological comparison. European journal of nuclear medicine and molecular imaging. Jul; 2004 31(7):995–1004. [PubMed: 14985863]

85. Lee WH, Chung YA, Seo YY, et al. Alterations of regional cerebral blood flow in major depressive disorder. Nuclear Medicine and Molecular Imaging. Apr; 2009 43(2):107–111.

86. Ye T, Peng J, Nie B, et al. Altered functional connectivity of the dorsolateral prefrontal cortex in first-episode patients with major depressive disorder. European journal of radiology. Dec; 2012 81(12):4035–4040. [PubMed: 22939367]

87. Vasic N, Walter H, Sambataro F, Wolf RC. Aberrant functional connectivity of dorsolateral prefrontal and cingulate networks in patients with major depression during working memory processing. Psychological medicine. Jun; 2009 39(6):977–987. [PubMed: 18845009]

88. Paelecke-Habermann Y, Pohl J, Leplow B. Attention and executive functions in remitted major depression patients. Journal of affective disorders. Dec; 2005 89(1-3):125–135. [PubMed: 16324752]

89. Fossati P, Ergis AM, Allilaire JF. Executive functioning in unipolar depression: a review. L'Encephale. Mar-Apr;2002 28(2):97–107.

90. Mayberg HS, Brannan SK, Mahurin RK, et al. Cingulate function in depression: a potential predictor of treatment response. Neuroreport. Mar 3; 1997 8(4):1057–1061. [PubMed: 9141092]

91. Auer DP, Putz B, Kraft E, Lipinski B, Schill J, Holsboer F. Reduced glutamate in the anterior cingulate cortex in depression: an in vivo proton magnetic resonance spectroscopy study. Biological psychiatry. Feb 15; 2000 47(4):305–313. [PubMed: 10686265]

92. Drevets WC. Neuroimaging and neuropathological studies of depression: implications for the cognitive-emotional features of mood disorders. Current opinion in neurobiology. Apr; 2001 11(2):240–249. [PubMed: 11301246]

93. Drevets WC, Price JL, Simpson JR Jr, et al. Subgenual prefrontal cortex abnormalities in mood disorders. Nature. Apr 24; 1997 386(6627):824–827. [PubMed: 9126739]

94. Drevets WC. Prefrontal cortical-amygdalar metabolism in major depression. Annals of the New York Academy of Sciences. Jun 29.1999 877:614–637. [PubMed: 10415674]

95. Drevets WC, Videen TO, Price JL, Preskorn SH, Carmichael ST, Raichle ME. A functional anatomical study of unipolar depression. The Journal of neuroscience : the official journal of the Society for Neuroscience. Sep; 1992 12(9):3628–3641. [PubMed: 1527602]

96. Perlman G, Simmons AN, Wu J, et al. Amygdala response and functional connectivity during emotion regulation: a study of 14 adolescents with depression. Journal of affective disorders. Jun; 2012 139(1):75–84. [PubMed: 22401827]

97. Cardinal RN, Parkinson JA, Hall J, Everitt BJ. Emotion and motivation: the role of the amygdala, ventral striatum, and prefrontal cortex. Neuroscience and biobehavioral reviews. May; 2002 26(3): 321–352. [PubMed: 12034134]

98. Craig AD. How do you feel--now? The anterior insula and human awareness. Nature reviews Neuroscience. Jan; 2009 10(1):59–70.

99. Carter CS, Botvinick MM, Cohen JD. The contribution of the anterior cingulate cortex to executive processes in cognition. Reviews in the neurosciences. 1999; 10(1):49–57. [PubMed: 10356991]

100. Yang TT, Simmons AN, Matthews SC, et al. Adolescents with depression demonstrate greater subgenual anterior cingulate activity. Neuroreport. Mar 4; 2009 20(4):440–444. [PubMed: 19218875]

101. Johansen-Berg H, Gutman DA, Behrens TE, et al. Anatomical connectivity of the subgenual cingulate region targeted with deep brain stimulation for treatment-resistant depression. Cerebral cortex (New York, NY : 1991). Jun; 2008 18(6):1374–1383.

102. Neumeister A, Nugent AC, Waldeck T, et al. Neural and behavioral responses to tryptophan depletion in unmedicated patients with remitted major depressive disorder and controls. Archives of general psychiatry. Aug; 2004 61(8):765–773. [PubMed: 15289275]

103. Hasler G, Fromm S, Carlson PJ, et al. Neural response to catecholamine depletion in unmedicated subjects with major depressive disorder in remission and healthy subjects. Archives of general psychiatry. May; 2008 65(5):521–531. [PubMed: 18458204]

104. Holthoff VA, Beuthien-Baumann B, Zundorf G, et al. Changes in brain metabolism associated with remission in unipolar major depression. Acta psychiatrica Scandinavica. Sep; 2004 110(3): 184–194. [PubMed: 15283738]

105. Mayberg HS, Brannan SK, Tekell JL, et al. Regional metabolic effects of fluoxetine in major depression: serial changes and relationship to clinical response. Biological psychiatry. Oct 15; 2000 48(8):830–843. [PubMed: 11063978]

106. Drevets WC, Bogers W, Raichle ME. Functional anatomical correlates of antidepressant drug treatment assessed using PET measures of regional glucose metabolism. European neuropsychopharmacology : the journal of the European College of Neuropsychopharmacology. Dec; 2002 12(6):527–544. [PubMed: 12468016]

107. Nobler MS, Oquendo MA, Kegeles LS, et al. Decreased regional brain metabolism after ect. The American journal of psychiatry. Feb; 2001 158(2):305–308. [PubMed: 11156816]

108. Kennedy SH, Giacobbe P, Rizvi SJ, et al. Deep brain stimulation for treatment-resistant depression: follow-up after 3 to 6 years. The American journal of psychiatry. May; 2011 168(5): 502–510. [PubMed: 21285143]

109. Holtzheimer PE, Kelley ME, Gross RE, et al. Subcallosal cingulate deep brain stimulation for treatment-resistant unipolar and bipolar depression. Archives of general psychiatry. Feb; 2012 69(2):150–158. [PubMed: 22213770]

110. Phan KL, Wager T, Taylor SF, Liberzon I. Functional neuroanatomy of emotion: a meta-analysis of emotion activation studies in PET and fMRI. NeuroImage. Jun; 2002 16(2):331–348. [PubMed: 12030820]

111. Chen YH, Dammers J, Boers F, et al. The temporal dynamics of insula activity to disgust and happy facial expressions: a magnetoencephalography study. NeuroImage. Oct 1; 2009 47(4): 1921–1928. [PubMed: 19442746]

112. Zeki S, Romaya JP. Neural correlates of hate. PloS one. 2008; 3(10):e3556. [PubMed: 18958169]

113. Surguladze SA, El-Hage W, Dalgleish T, Radua J, Gohier B, Phillips ML. Depression is associated with increased sensitivity to signals of disgust: a functional magnetic resonance imaging study. Journal of psychiatric research. Oct; 2010 44(14):894–902. [PubMed: 20307892]

114. Dalby RB, Elfving B, Poulsen PH, et al. Plasma brain-derived neurotrophic factor and prefrontal white matter integrity in late-onset depression and normal aging [published online January 27, 2013]. Acta Psychiatr Scand. 201310.1111/acps.12085

115. George MS, Ketter TA, Parekh PI, Horwitz B, Herscovitch P, Post RM. Brain activity during transient sadness and happiness in healthy women. The American journal of psychiatry. Mar; 1995 152(3):341–351. [PubMed: 7864258]

116. Reiman EM, Lane RD, Ahern GL, et al. Neuroanatomical correlates of externally and internally generated human emotion. The American journal of psychiatry. Jul; 1997 154(7):918–925. [PubMed: 9210741]

117. Wang, J.; Rao, H.; Wetmore, GS., et al. Perfusion functional MRI reveals cerebral blood flow pattern under psychological stress; Proceedings of the National Academy of Sciences of the United States of America; Dec 6 2005; p. 17804-17809.

118. Herrington JD, Taylor JM, Grupe DW, Curby KM, Schultz RT. Bidirectional communication between amygdala and fusiform gyrus during facial recognition. NeuroImage. Jun 15; 2011 56(4):2348–2355. [PubMed: 21497657]

119. Konarski JZ, McIntyre RS, Grupp LA, Kennedy SH. Is the cerebellum relevant in the circuitry of neuropsychiatric disorders? Journal of psychiatry and neuroscience : JPN. May; 2005 30(3):178–186. [PubMed: 15944742]

120. Schmahmann JD. An emerging concept. The cerebellar contribution to higher function. Archives of neurology. Nov; 1991 48(11):1178–1187. [PubMed: 1953406]

121. Anand BK, Malhotra CL, Singh B, Dua S. Cerebellar projections to limbic system. Journal of neurophysiology. Jul; 1959 22(4):451–457. [PubMed: 13673296]

122. Heath RG, Dempesy CW, Fontana CJ, Myers WA. Cerebellar stimulation: effects on septal region, hippocampus, and amygdala of cats and rats. Biological psychiatry. Oct; 1978 13(5):501–529. [PubMed: 728506]

123. Vilensky JA, van Hoesen GW. Corticopontine projections from the cingulate cortex in the rhesus monkey. Brain research. Feb 2; 1981 205(2):391–395. [PubMed: 7470872]

124. Schmahmann JD, Sherman JC. The cerebellar cognitive affective syndrome. Brain : a journal of neurology. Apr; 1998 121(Pt 4):561–579. [PubMed: 9577385]

125. Levisohn L, Cronin-Golomb A, Schmahmann JD. Neuropsychological consequences of cerebellar tumour resection in children: cerebellar cognitive affective syndrome in a paediatric population. Brain : a journal of neurology. May; 2000 123(Pt 5):1041–1050. [PubMed: 10775548]

126. Liotti M, Mayberg HS, McGinnis S, Brannan SL, Jerabek P. Unmasking disease-specific cerebral blood flow abnormalities: mood challenge in patients with remitted unipolar depression. The American journal of psychiatry. Nov; 2002 159(11):1830–1840. [PubMed: 12411216]

127. Liu CH, Ma X, Li F, et al. Regional homogeneity within the default mode network in bipolar depression: a resting-state functional magnetic resonance imaging study. PloS one. 2012; 7(11):e48181. [PubMed: 23133615]

128. Guo W, Liu F, Dai Y, et al. Decreased interhemispheric resting-state functional connectivity in first-episode, drug-naive major depressive disorder. Progress in neuro-psychopharmacology and biological psychiatry. Mar 5.2013 41:24–29. [PubMed: 23159796]

129. Liu L, Zeng LL, Li Y, et al. Altered cerebellar functional connectivity with intrinsic connectivity networks in adults with major depressive disorder. PloS one. 2012; 7(6):e39516. [PubMed: 22724025]

130. Ma Q, Zeng LL, Shen H, Liu L, Hu D. Altered cerebellar-cerebral resting-state functional connectivity reliably identifies major depressive disorder. Brain research. Feb 7.2013 1495:86–94. [PubMed: 23228724]

131. Mayberg HS, Lewis PJ, Regenold W, Wagner HN Jr. Paralimbic hypoperfusion in unipolar depression. Journal of nuclear medicine : official publication, Society of Nuclear Medicine. Jun; 1994 35(6):929–934.

132. Aguirre GK, Detre JA, Zarahn E, Alsop DC. Experimental design and the relative sensitivity of BOLD and perfusion fMRI. NeuroImage. Mar; 2002 15(3):488–500. [PubMed: 11848692]

133. Viviani R, Messina I, Walter M. Resting state functional connectivity in perfusion imaging: correlation maps with BOLD connectivity and resting state perfusion. PloS one. 2011; 6(11):e27050. [PubMed: 22073252]

134. Chuang KH, van Gelderen P, Merkle H, et al. Mapping resting-state functional connectivity using perfusion MRI. NeuroImage. May 1; 2008 40(4):1595–1605. [PubMed: 18314354]

135. Liu J, Hao Y, Du M, et al. Quantitative cerebral blood flow mapping and functional connectivity of postherpetic neuralgia pain: a perfusion fMRI study. Pain. Jan; 2013 154(1):110–118. [PubMed: 23140909]

136. Mayberg HS. Modulating limbic-cortical circuits in depression: targets of antidepressant treatments. Seminars in clinical neuropsychiatry. Oct; 2002 7(4):255–268. [PubMed: 12382208]

137. Liu TT, Brown GG. Measurement of cerebral perfusion with arterial spin labeling: Part 1. Methods. J Int Psychol Soc. 2007; 23:517–525.

138. Chen Y, Wang DJ, Detre JA. Test-retest reliability of arterial spin labeling with common labeling strategies. Journal of magnetic resonance imaging : JMRI. Apr; 2011 33(4):940–949. [PubMed: 21448961]

139. Gevers S, van Osch MJ, Bokkers RP, et al. Intra- and multicenter reproducibility of pulsed, continuous and pseudo-continuous arterial spin labeling methods for measuring cerebral perfusion. Journal of cerebral blood flow and metabolism : official journal of the International Society of Cerebral Blood Flow and Metabolism. Aug; 2011 31(8):1706–1715. [PubMed: 21304555]
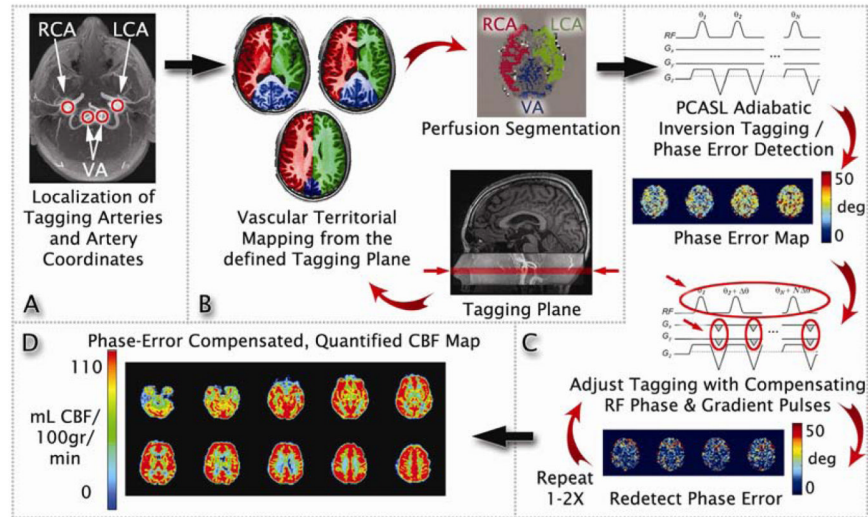
Figure 1.
A graphical depiction of the prescans and pseudocontinuous arterial spin labeling (PCASL) scan in the optimized PCASL method. Note: See Image Acquisition under Method for more details). A series of time of flight (TOF) images were acquired to generate a high-resolution view of the main feeding arteries to the brain. The coordinates of the tagging plane and feeding arteries are then saved into a configuration file (Figure 1A). The spatial coordinates of the feeding arteries from the TOF scan are used to image the vascular territories via vessel-encoded arterial spin labeling (ASL) (Figure 1B). Lastly, up to 2 multiphase PCASL (MP-PCASL) scans are used to estimate phase tracking errors in each of the territory masks acquired from the vascular territorial imaging scan (Figure 1C). Note that the first MP-PCASL scan is used to measure the uncorrected phase errors while the second MP-PCASL scan is to verify that the errors are minimized after modulating the radiofrequency phase and in-plane gradients to the PCASL pulse train. If the phase tracking errors from the first MP-PCASL scan are less than 20°, then the second MP-PCASL scan is skipped (Figure 1C). The optimized global radio frequency phase and in-plane gradients determined by the MP-PCASL scan(s) are then applied to the tagging module for the PCASL scan (Figure 1D). LCA=left carotid artery; RCA=right carotid artery; VA=vertebral artery. From Shin *et al.* Pseudocontinuous arterial spin labeling with optimized tagging efficiency. Magnetic resonance in medicine. Oct 2012;68(4):1135-1144.[39] Reprinted with permission from John Wiley and Sons.
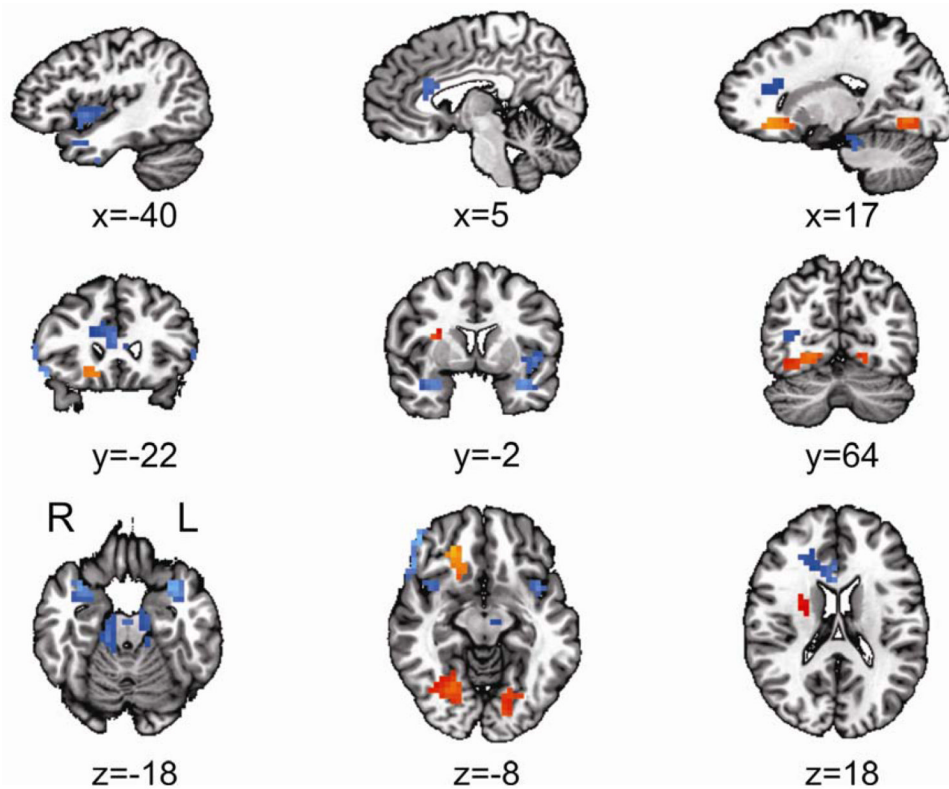
Figure 2.
The voxel-based whole brain analysis revealed 12 clusters with significantly different regional cerebral blood flow (rCBF) levels in major depressive disorder (MDD) compared with healthy controls (HCL) (orange=increased, blue=decreased). Note: Eight clusters revealed significantly lower mean rCBF in the MDD compared to the HCL group: bilateral parahippocampal gyri/insula, right inferior frontal/dorsolateral prefrontal cortex (Brodmann area [BA] 44/45 and BA46), right anterior cingulate cortex, right middle occipital gyrus, left inferior temporal gyrus, and bilateral cerebellum. Four clusters revealed significantly higher mean rCBF in the MDD compared to HCL group: right subcallosal cingulate, right putamen, and bilateral fusiform gyrus. All locations are reported in Talairach coordinates (see Results and Table 1 for more details). Results are overlaid on a standardized Talairach template. Significance of each cluster is p<0.05 (see Whole Brain Analysis under Method for more details). L=left; R=right.
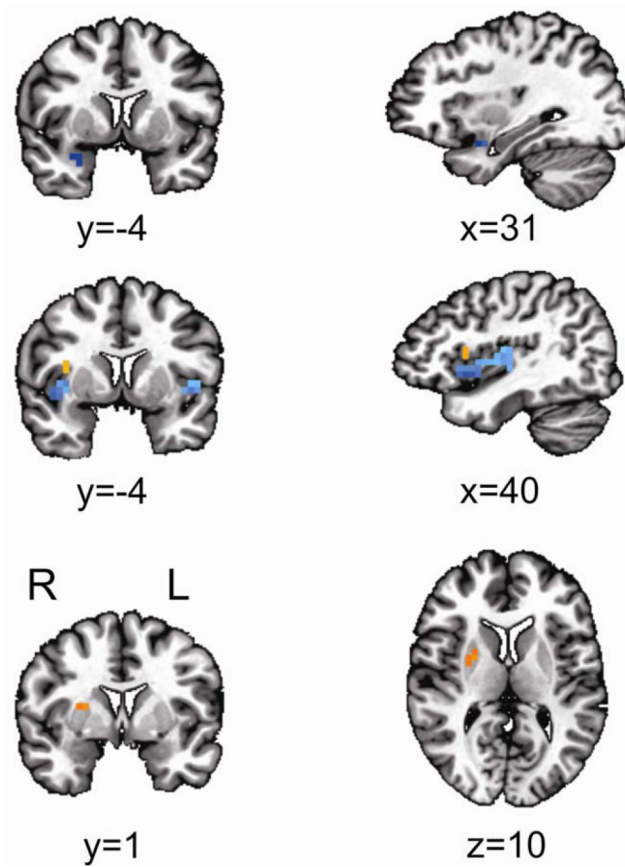
Figure 3.
The region-of-interets (ROI) analysis revealed 5 clusters with significantly different regional cerebral blood flow (rCBF) levels in major depressive disorder (MDD) compared with healthy controls (HCL) (orange=increased, blue=decreased). Note: Three clusters with significantly lower rCBF levels in MDD compared with HCL: right amygdala (top row) and bilateral insula (middle row). Two clusters revealed significantly higher rCBF levels in MDD compared with HCL: right superior insula (Brodmann Area [BA] 13; middle row) and right putamen/lentiform nucleus (bottom row). All locations are reported in Talairach coordinates (see Results and Table 2 for more details). Results are overlaid on a standardized Talairach template. Significance of each cluster is p<0.05 (see Region-of-Interest Analysis under Method for more details). L=left; R=right.

Table 1

Significant Clusters From the Voxel-Based Whole Brain Analysis

Cluster	MDD rCBF (mL/100 g/min)	HCL rCBF (mL/100 g/min)	t-value (df=49)	p-value (corrected)	# of voxels	x	y	Z
L Parahippocampal Gyrus/Insula	51.8 ± 2.7	69.7 ± 2.9	−4.51	***	85	−40	−9	−8
R Inferior Frontal Gyrus/Dorsolateral Prefrontal (BA44/45 and BA46)	36.8 ± 2.5	57.0 ± 3.5	−4.66	***	85	52	−29	1
R Fusiform Gyrus	57.8 ± 2.1	47.8 ± 1.8	3.63	***	48	24	63	−6
L Cerebellum	36.8 ± 2.7	50.5 ± 2.7	−3.60	***	47	−13	17	−19
R Anterior Cingulate Cortex	36.3 ± 2.4	50.1 ± 4.2	−2.82	***	46	8	−22	19
L Inferior Temporal Gyrus	29.5 ± 3.1	46.3 ± 3.7	−3.50	***	40	−52	11	−27
R Cerebellum	39.3 ± 2.2	52.8 ± 2.7	−3.86	***	40	13	25	−19
R Parahippocampal Gyrus/Insula	50.9 ± 3.7	69.0 ± 4.0	−3.32	***	37	35	−7	−14
L Fusiform Gyrus	70.3 ± 2.4	60.2 ± 2.1	3.17	***	34	−15	79	−4
R Subcallosal Cingulate Gyrus	63.0 ± 5.8	44.0 ± 2.5	3.05	**	26	17	−21	−10
R Putamen	45.3 ± 2.9	36.1 ± 1.8	2.69	*	24	27	−3	16
R Middle Occipital Gyrus	37.1 ± 1.6	46.9 ± 2.1	3.70	*	21	34	62	10

Note: See also Results and Figure 2. Extracted values for major depressive disorder (MDD) and healthy controls (HCL) reported in regional cerebral blood flow (rCBF) (mean ± standard error of mean [SEM]). Reported significance values are at the clusterwise level (see Whole Brain Analysis under Method for more details). Locations reported according to center of mass of cluster in Talairach coordinates (radiological convention). BA=Brodmann area; df=degrees of freedom; g=grams; L=left; min=minute; mL=milliliters; R=right.

*
p<0.05,

**
p< 0.01,

***
p<0.001.

Table 2

Significant Clusters From the Region-of-Interest (ROI) Analysis

Cluster	MDD rCBF (mL/100 g/min)	HCL rCBF (mL/100 g/min)	t-value (df=49)	p-value (corrected)	# of voxels	x	y	z
R Insula	70.85 ± 3.14	80.10 ± 3.26	−2.04	***	51	40	−3	1
L Insula	64.23 ± 3.18	79.93 ± 2.93	−3.64	**	11	−44	−5	1
R Superior Insula (BA13)	69.08 ± 2.53	61.06 ± 2.94	2.06	**	12	35	−7	13
R Putamen/Lentiform Nucleus	53.68 ± 2.29	45.99 ± 2.70	2.16	*	4	24	1	12
R Amygdala	43.12 ± 3.68	62.08 ± 5.43	−2.87	*	4	28	−2	−17

Note: See also Results and Figure 3. Extracted values for major depressive disorder (MDD) and healthy controls (HCL) reported in regional cerebral blood flow (rCBF) (mean ± standard error of mean [SEM]). Reported significance values are at the clusterwise level (see Region-of-Interest Analysis under Method for more details). Locations reported according to center of mass of cluster in Talairach coordinates (radiological convention). BA=Brodmann area; df=degrees of freedom; g=grams; L=left; min=minute; mL=milliliters; R=right;

*
  $p<0.05$,

**
  $p<0.01$,

***
  $p<0.001$.